JOURNAL OF SOLID STATE CHEMISTRY 64, 305–321 (1986)

Synthesis and Properties of Low-Dimensional Metal Chalcogenides

JEAN ROUXEL

U.A. 279, CNRS, University of Nantes 2, rue la Houssinière, F-44072 Nantes Cedex, France

Received September 13, 1985

The search of new one-dimensional (1D) conducting compounds cannot be conducted only from geometrical considerations, for example, by looking at the various ways to associate coordination polyhedra to form chains. Two other conditions must be fulfilled: a condition external to the chain that implies that they be stable with respect to one another, in relation with a certain ionicity of the network, and an internal condition on cation–cation direct interaction to obtain metallic conductivity. A more empirical way to start with consists in considering the charge density wave type phenomenon and to see the various possible evolutions from a given material. These considerations are illustrated on the basis of a continuous evolution from di- to trichalcogenides, then halogenotetrachalcogenides, doped materials, and finally waved 1D compounds. © 1986 Academic Press, Inc.

During the past 10 years, low-dimensional solid have been the pillar of numerous studies in physics and chemistry of solids. They have been considered as host structures in intercalation chemistry. Also the structural anisotropy directly reflects in a strong anisotropy of the physical properties which may be of interest by itself (low-dimensional magnetism, for example), but the most striking physical properties are observed among low-dimensional compounds that are conductors. There, structural instabilities of the charge density wave type (CDW) may be observed in connection with a Fermi surface presenting large parallel sections.

In this paper we report recent attempts to synthesize new one-dimensional conductors in the series of niobium and tantalum chalcogenides.

I. Some General Features

The van der Waals gap that separates slabs or fibers in two-dimensional or one-dimensional materials is bonded on each side by atomic layers of the same nature. Besides geometrical factors, its width will depend on the electronegativity of these atoms. For a given structural type to be stable the bonding through the van der Waals gap must stabilize the structure against the repulsion between the same atomic layers situated on each side. In the case of oxides this repulsion is quite strong and very destabilizing. The rutile structure is observed in most of the MO_2 transition metal oxides and not the layered forms of the parent MS_2 chalcogenides. Layered oxides can exist only for the highest oxidation states of transition metals (less ionic character), if (OH^-)

0022-4596/86 $3.00

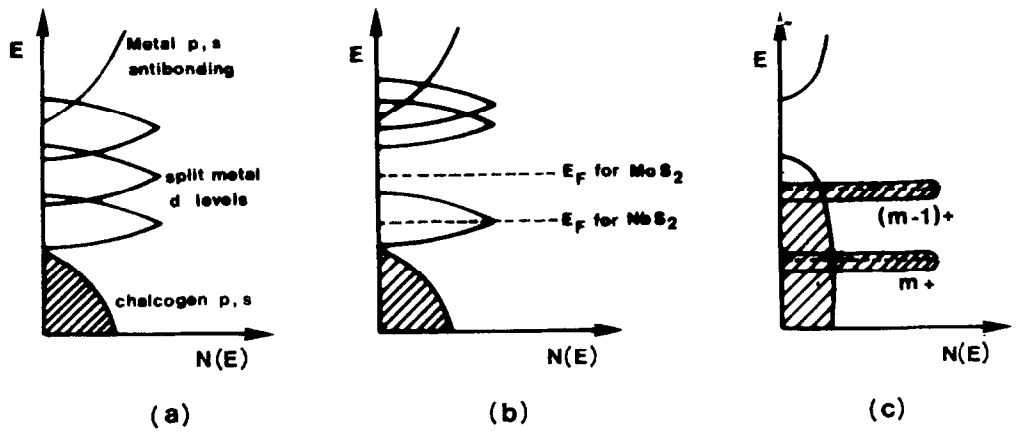

FIG. 1. Band schemes: (a) general feature, (b) particular case of NbS_2 (dz^2 band half-filled) and MoS_2 (dz^2 band filled), (c) situation at the end of a period (FeS_2).

groups are present allowing hydrogen bonds to stabilize the structures and also when extra cations are located between the slabs separating negative layers and introducing attractive coulombic forces. Between the too much ionic oxides and the quasimetallic tellurides, sulfides and selenides represent one of the most favorable domains in chemistry where 1D and 2D derivatives may be found.

To get a conductor we need direct interaction between populated cationic orbitals. This implies that supplementary conditions concerning the geometry of the structure and the electronic configuration of the elements are fulfilled. Between a valence band essentially *sp* anionic in character and an antibonding band mainly formed from the corresponding cationic levels, the d orbitals of the metal, split by the crystal field, play an essential role concerning the physical properties (Fig. 1). A maximum oxidation state of four is generally observed leading to d^0 configuration and no electronic conductivity in the case of the IVA elements. A d^1 configuration in the case of vanadium, niobium, and tantalum is responsible of the metallic behavior of the corresponding dichalcogenides. These VA elements represent the most favorable case. Immediately after, with a d^2 configuration, in the case where a symmetry splitting leads to a lowering of a dz^2 band, no electrical conductivity will result and this is the case of MoS_2 or WS_2. In addition, on going to the right of the periodic table the expansion of the *d* orbitals decreases, reducing the chance of overlapping and leading to localized levels. At the same time the *d* level are progressively lowered and at a certain point will enter the *sp* anionic valence band. If a filled *d* level enters the valence band there is no drastic change in the electrical properties. But if an empty *d* level is in this situation, it will fill up at the expense of the anionic *sp* band, at the higher part of which holes appear (*1*). This is the case upon reduction of Fe^{3+} into Fe^{2+} in pyrite or marcasite with the occurrence of $(S_2)^{2-}$ pairs in combination with positive holes.

Now, starting with the use of tetrahedra, octahedra, and trigonal prisms as modules in a construction game, one can theoretically imagine various ways of building 1D structures. By sharing corners constructions do not allow direct cation–cation interactions and have to be rejected. The sharing of edges allows such interactions,

but in fact, up to now, 1D conducting systems are concerned with the most favorable case, which is that of chains formed through a face-sharing arrangement. Classical examples are now those of $NbSe_3$, of the tetrachalcogenides of the $(MSe_4)_n$-halogen type, and of Krogmann's salts and related derivatives that show still more open structures. The metallic chain hence is spread amid a frame of ligands which is relatively covalent and rather open so as to lessen the potential variations.

In fact, when trying to design new 1D conductors a purely predictive approach proves quickly limited. As far as the stability of 1D structures is concerned, two conditions, largely contradictory have to be fulfilled:

(i) These chains must form with respect to each other a stable arrangement. Now the structure will be the more 1D if an increase of the ionic character will introduce repulsive actions between chains. But this will induce some instability for the structure and the compound may become unstable.

(ii) Each chain must also be stable and this implies that cation–cation repulsions be sufficiently shielded in spite of the necessity to have otherwise opened structure to allow electronic delocalization. Actually, the more 1D the structure the more this condition will be difficult to fulfill.

Also it is often convenient to look at the phenomena itself and to act from a given material. This approach may also allow one to obtain quite new structures.

Here the material is $NbSe_3$ (*2*) and the phenomenon is the charge density wave.

II. Using CDWs Properties to Design New 1D Compounds Starting from $NbSe_3$

CDWs are coupled distortions of both the density of conduction electrons and the underlying lattice. At a point characterized by a position vector $\mathbf{r}$ along a metallic chain the electronic density appears as

$$\rho(\mathbf{r}) = \rho_o[1 + \alpha \cos(\mathbf{q} \cdot \mathbf{r} + \phi)],$$

where $\mathbf{q}$, the wave vector of the modulation, is equal to twice the Fermi vector, and α expresses the amplitude variation relative to ρ_o, the average value in the absence of any fluctuation. ϕ is the phase. Such instabilities, which are due to the particular shape of the Fermi surface with large parallel sections (nesting condition), are possible because the opening of a gap in the Fermi surface at those portions which can nest leads to a gain in electronic energy which compensates for the cost in strain energy associated with the distortion.

The phenomenon provides by itself the means of its characterization. Electron diffraction techniques allow one to visualize the superstructure and to measure the q vector. Typical electrical curves show an increase in resistivity in relation with the decrease in area of the Fermi surface at the transition. Hall effects measurements give indications about the loss of carriers at the transition but have to be considered with prudence because there is a change in the mobility anisotropy at the same time, due to a change in the structure. Specific heat measurements are more adapted to determine the loss of carriers at the transition.

These pictures represent what can be called the static situation of a CDW as known through transition metal dichalcogenides (*3*). $NbSe_3$ brought a very important new point. This material presents two CDWs occurring at 145 and 59 K, respectively. But its most striking properties are in fact the nonlinear transport properties under low electrical fields and the behavior at microwave frequencies which are observed below the two independent CDW transition (*4*). These properties have been associated with a motion of the CDWs which were initially pinned to the lattice. A sufficient electric field is necessary to over-

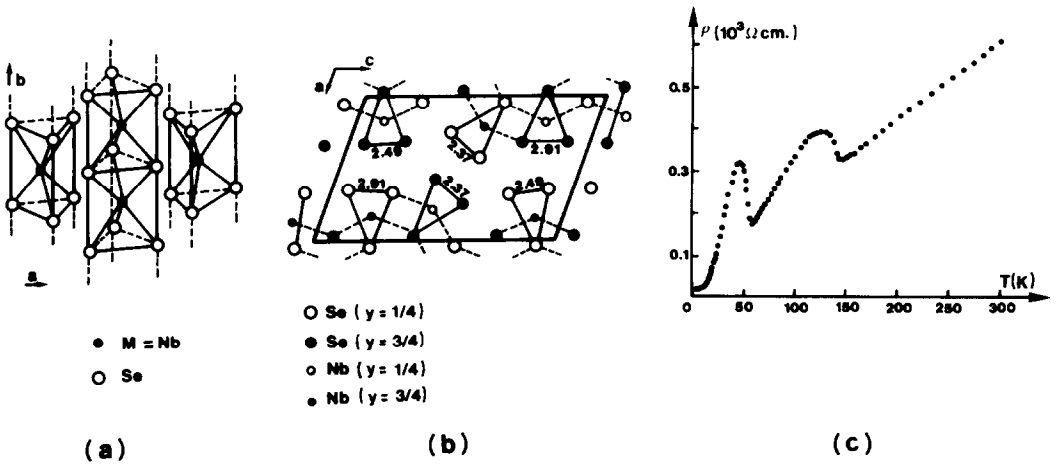

FIG. 2. (a) The three types of chains and (b) their relative arrangement in $NbSe_3$. (c) Resistivity curve.

come the pinning energy which depends on various factors such as interchain coupling, chemical impurities, gap to commensurability with the underlying lattice. A better understanding of these phenomena is largely dependent on the work of the chemist. Indeed the chemist can act upon these various factors and we tried to give some answers through:

(i) the search for materials more 1D in character

(ii) the search for polytypes

(iii) the effect of doping

(iv) the preparation of new series.

All these possibilities stem from a critical discussion of the material $NbSe_3$. Three different chains are found in its structure (Fig. 2) according to three different values taken by the Se—Se bond length in their triangular basis (respectively, 2.37, 2.48, 2.91 Å). The two CDWs occur in the two first types of chains, the third chain being probably an insulating one. However, the transverse distance between one metal and chalcogen atoms belonging to neighboring chains (translated from $b/2$) are not long enough to exclude any bonding. Vibrational spectroscopy studies show that the strength of these lateral Nb—Se bonds is a substantial fraction (0.15 to 0.28) of that of the intrachain M—X bond (*5*). $NbSe_3$ is not a perfect 1D compound, only portions of the Fermi surface nest and it remains semimetallic below the transitions.

But let us substitute tantalum for niobium and sulfur for selenium. Due to the more electropositive character of tantalum and to the more electronegative character of sulfur, TaS_3, if stable, will be more ionic and consequently much more one-dimensional than $NbSe_3$. This explains why, in TaS_3 which was known indeed (*6*), the transition goes as far as a metal–insulator transition. The nesting condition is much more perfectly fulfilled by the Fermi surface of TaS_3. In addition electron diffraction observations show a pretransitional effect manifested by diffuse lines that will condense into spots at the transition. It means that above the transition the CDW modulation exists dynamically but with phase incoherence between chains.

Just as in most two-dimensional compounds, in which slabs may behave more or less as independent units, polytypism is expected in the case of 1D derivatives and

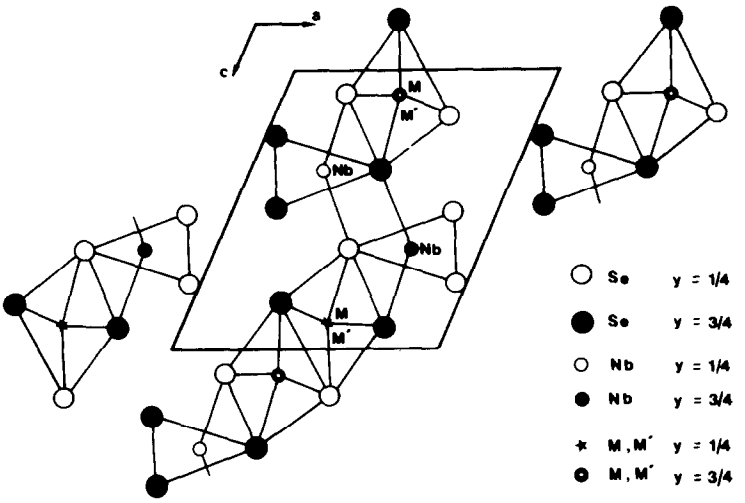

FIG. 3. $FeNb_3Se_{10}$ structural type.

particularly in the case of trichalcogenides. It should associate the various chains or fibers in new arrangements. We never observed any polytype in the case of $NbSe_3$ itself when trials were successful in the case of TaS_3. Besides the already known orthorhombic form which presents a metal to insulator transition at 210 K (*7*), we prepared a monoclinic variety which shows two transitions, i.e., a metal-to-insulator transition at 240 K and another transition in the semiconducting state at 168 K (*8*). The important points brought by this material concern (i) a comparison between the two polytypes, orthorhombic TaS_3 having a commensurate transition and monoclinic TaS_3 two incommensurate transitions (Table I), and (ii) a comparison between monoclinic TaS_3 and $NbSe_3$ with two conducting chains and an insulating one in each case but with different couplings.

A way to modify the electronic density and the properties of low-dimensional compounds is to change the chemical composition either by atomic substitutions in the chains or by intercalation between them. Only very small amounts of other atoms, particularly tantalum, have been substituted for niobium in $NbSe_3$. These atoms act as chemical defects which can be related to the pinning mechanism of CDWs. From experiments involving iron, a new compound was found with the chemical formulation $FeNb_3Se_{10}$ (*9*). Two types of chains (Fig. 3) are present in the structure, running along the *b* axis of the monoclinic unit cell. One of them corresponds to a trigonal prismatic frame of selenium atoms around niobium, identical to the chain with the shortest Se—Se bond length in $NbSe_3$. The second chain develops an octahedral

TABLE I

q VECTORS OF THE DISTORTIONS IN $NbSe_3$, TaS_3, AND $FeNb_3Se_{10}$

$NbSe_3$ (Monoclinic)	T_2 = 59 K	T_1 = 145 K	$T > 145$ K
	0, 0.241, 0, ½, 0.259, ½	0, 0.243, 0	No diffuse lines
TaS_3 (Monoclinic)	T_2 = 160 K	T_2 = 240 K	$T > 240$ K
	0, 0.254, 0, ½, 0.245, ½	0, 0.254, 0	Diffuse lines
TaS_3 (Orthorhombic)	T = 210 K ½, ½, ½		
$FeNb_3Se_{10}$	$T \leq 140$ K q(0., 0.27(1), 0)		

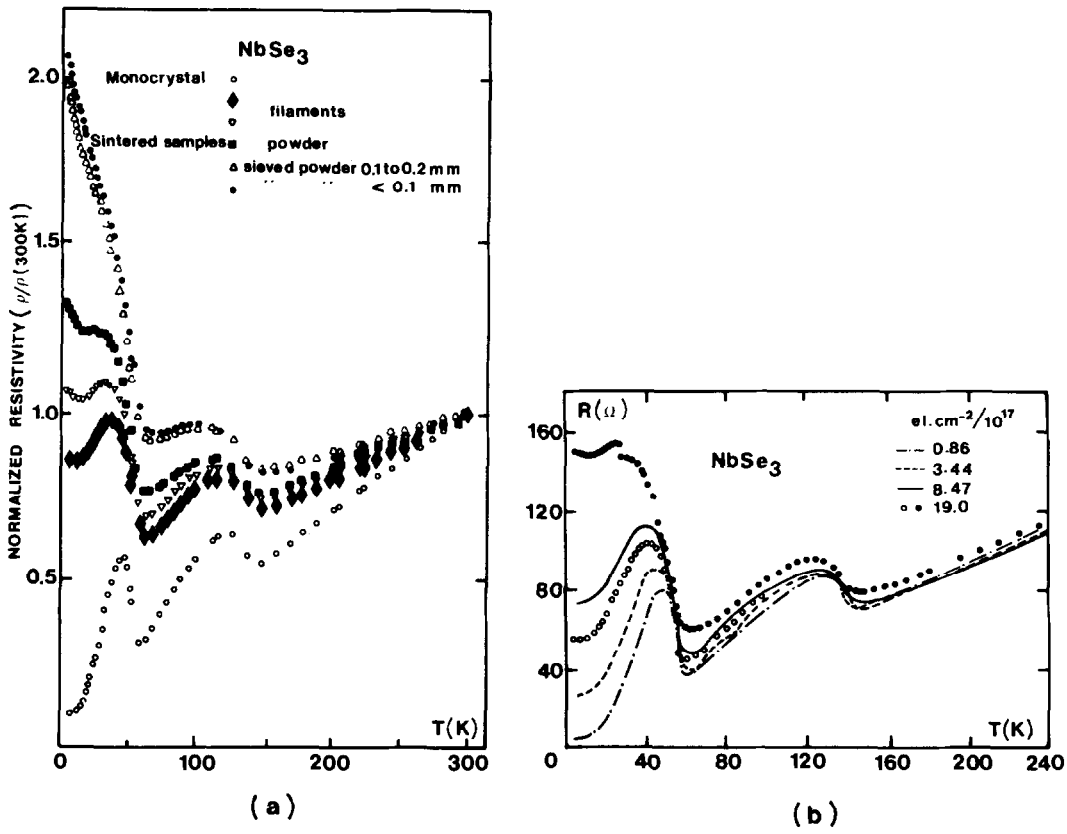

FIG. 4. Resistivity curves of $NbSe_3$ sintered samples (a) or with irradiation defects (b).

distribution of selenium atoms around both niobium and iron in variable proportions, which allows some nonstoichiometry. This situation can be regarded as the result of condensations in a given structure of various chains, each of them corresponding to the usual situation of a given element (octahedral, trigonal prismatic). A nice extension of this proposition is to be found in the work of Ibers and co-workers with square planar coordination of Pd in other chains and a great flexibility of composition according to the ratio between different types of chains (*10*).

The trigonal prismatic chain in $FeNb_3Se_{10}$ retained the properties it has in $NbSe_3$. A metal to nonmetal transition appears at 140 K with a distortion having the same distortion vector as the first CDW in $NbSe_3$. Indirectly this is a proof that this CDW was really seated in the corresponding chain in $NbSe_3$.

Before leaving trichalcogenides let us consider three additional points that are of importance concerning chemical synthesis. The first point concerns the dependence of the electrical behavior on the quality of crystals. A common feature (Fig. 4) among the resistivity curves for samples containing chemical impurities, irradiation defects, or sintered polycrystals is that the resistivity increases sharply at lower temperatures. A similar behavior is found on $NbSe_3$ samples prepared under pressure. Besides a residual impurity effect that can be seen on the figure these features seem to be associ-

ated with a shortening of the lengths of conducting chains, since a similar behavior is observed when the conductivity is measured on samples made of small grains.

The second point that merits underlining is the variable length of the chalcogen pairs in these materials. From a chemical point of view, this is an important feature. The Se—Se pair behaves as an electron reservoir, which governs indirectly the electronic density available along the metallic chains and consequently the electrical properties of these chains.

The third point is that substitution in chains or slabs is not always easy to perform chemically. We wish to emphasize the particular importance of the electronic configuration of the cation to be substituted. Isoelectronic substitution can be performed but a very important thing is the crystal field stabilization in the corresponding site. Let us consider the particular case of the MPS_3 series. These compounds exhibit a 2D structure built up from TiS_2 type slabs in which the octahedral sites normally occupied by titanium are shared by the M^{2+} cation in the proportion of two-thirds and (P—P) pairs in the proportion of one-third. Mn^{2+}, Zn^{2+}, Cd^{2+} with a isotropic electronic distribution, and no crystal field stabilization, can be easily substituted (*11*). For example, at room temperature:

$$MnPS_3 + 2x(K^+\ Cl^-)_{aqueous} \rightarrow M_{1-x}K_{2x}PS_3 + xMn^{2+} + 2xCl^-$$

Fe^{2+} in $FePS_3$ can be substituted with the additional help of a complexing reagent (EDTA). Ni^{2+} cannot be substituted. The thermal agitation of the cations gives already some indications on possible substitutions (Table II).

TABLE II

THERMAL AGITATION FACTORS IN THE MPS_3 SERIES

	M					
	Mn	Fe	Co	Ni	Zn	Cd
B_{eq} (Å²)	1.22	1.11	1.05	0.75	—	1.74
d configuration	d^5 $t_{2g}^3e_g^2$	d^6 $t_{2g}^4e_g^2$	d^7 $t_{2g}^5e_g^2$	d^8 $t_{2g}^6e_g^2$	d^{10} $t_{2g}^6e_g^4$	d^{10} $t_{2g}^6e_g^4$

III. Tetrachalcogenides

In the mineral VS_4 two anionic pairs, not just one as in trichalcogenides, are present in the structure. A $d_1 - d_1$ pairing gives a diamagnetic behavior to this vanadium(IV) derivative. Trials to prepare NbX_4 or TaX_4 were unsuccessful. But, adding an halogen, a complete series of new materials was found (*12*) with the general formulation $(MX_4)_nY$ (M = Nb, Ta; X = S, Se; Y = Br, I; n = 2, 3, 10/3, etc . . .). Single needle shaped crystals of these phases are obtained by mixing the elements in evacuated and sealed glass tubes at temperatures ranging from 400 to 550°C. The common structural type of these phases can be illustrated by considering $(NbSe_4)_3I$. With a tetragonal symmetry (*P4/mnc*) the structure is composed of $NbSe_4$ chains and iodine columns which are both parallel to the *c* axis. The metallic chains are widely separated: two niobium having the same *z* value, but belonging to different chains, are 6.70 Å apart. Along the chains Nb—Nb atomic positions alternate in the sequence of two long (3.25 Å) and one short (3.06 Å) distances. From one compound to another this sequence changes according to the amount of counterion (Table III). The second difference concerns the way the Se_4 rectangles, made of two true $(Se_2)^{2-}$ pairs (Se—Se ≈ 2.35 Å) and surrounding Nb or Ta in an antiprismatic manner, turn around the axis of the chains. Indeed the $[MSe_8]$ rectangular antiprisms are stacked along the *c* axis in a screw-like arrangement characterized by the relative position of the arrows pointing from the center to the middle of the edges (see Table III and Fig. 5). Every two adjacent $(Se_4)^{4-}$ units have a di-

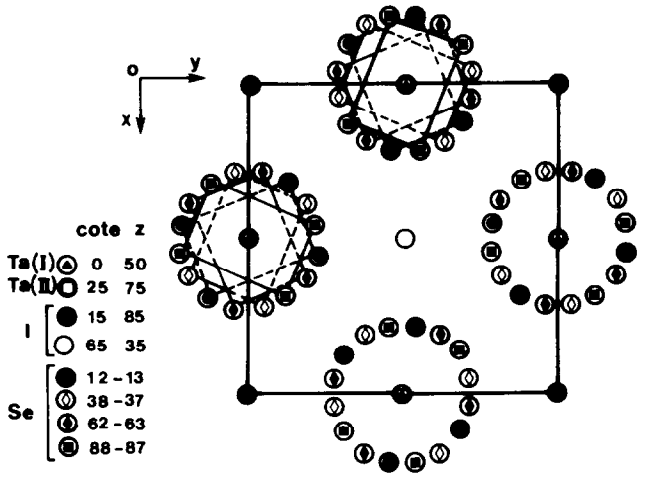

FIG. 5. $(MSe_4)_n$-halogen structural type illustrated by $(TaSe_4)_2I$.

hedral angle θ of about 45°. This is mainly due to their occupied π and π^* orbitals. First the overlap between such adjacent orbitals is minimized, therefore minimizing repulsive interactions. Also at $\theta = 45°$, π and π^* orbitals provide symmetry-adapted orbitals which interact with all metal d orbitals except for dz^2. Along the chain the metal dz^2 orbitals form a narrow d band which governs the electronic properties of the system (*13*). If the role of the halogen is neglected each $[MSe_4]$ chain has an M^{4+} (d^1) metal ion at the center of every (Se_8) rectangular antiprism. Then each iodine takes about one electron and the average number of d electrons on each metal would be $(n - 1)/n$. The corresponding filling of the dz^2 band is $f = (n - 1)/2n$ possibly leading to a distortion increasing the repeat distance by a factor of $1/f$. This first approach suggests that $(NbSe_4)_3I$, $(NbSe_4)_{10/3}I$, and $(TaSe_4)_2I$, for example, would have $\frac{1}{3}$, $\frac{7}{20}$, and $\frac{1}{4}$ filled dz^2 bands, respectively. As n increases the dz^2 band of $(MSe_4)_nI$ becomes closer to $\frac{1}{2}$ filled. Vanadium tetrasulfide constitutes finally an example of the $n \to \infty$ limit. It has a $2c$ insulating Peierls distortion. More precisely tight-binding band structure calculations have been performed. They are in rather good agreement with the observed distortions. For example, the calculations on $(TaSe_4)_2I$ lead to an estimation of $2k_F = 0.88\ c^*$ (*13*) and the distortion is observed at 0.94 c^* Ref. (*14*) and 0.91 c^* in Ref. (*15*).

TABLE III

METAL–METAL SEQUENCES OF BONDS IN $(MSe_4)_n$-HALOGEN PHASES

Compound	*M–M* sequence
$(NbSe_4)_3I$	$-Nb\overset{3.25}{-}Nb\overset{3.25}{-}Nb\overset{3.06}{-}Nb-$
$(NbSe_4)_{3.33}I$	$-Nb\overset{3.17}{-}Nb\overset{3.17}{-}Nb\overset{3.23}{-}Nb\overset{3.15}{-}Nb\overset{2.23}{-}Nb-$
$(TaSe_4)_2I$	$-Ta\overset{3.206}{-}Ta\overset{3.206}{-}Ta-$
$(TaSe_4)_3I$	(Same sequence as for $(NbSe_4)_3I$)
$(NbSe_4)_3Br$	$-Nb\overset{3.15}{-}Nb\overset{3.15}{-}Nb\overset{3.45}{-}Nb\overset{3.45}{-}Nb-$

This distortion, in $(TaSe_4)_2I$ appears at 263 K. It is manifested by a sharp peak (Fig. 6) in the logarithmic derivative curve $d\log(R/R_0)/d(1/T)$. The CDW origin is demonstrated by the depinning which is possible above a threshold field (*16, 17*). Typical nonlinear differential curves are then ob-

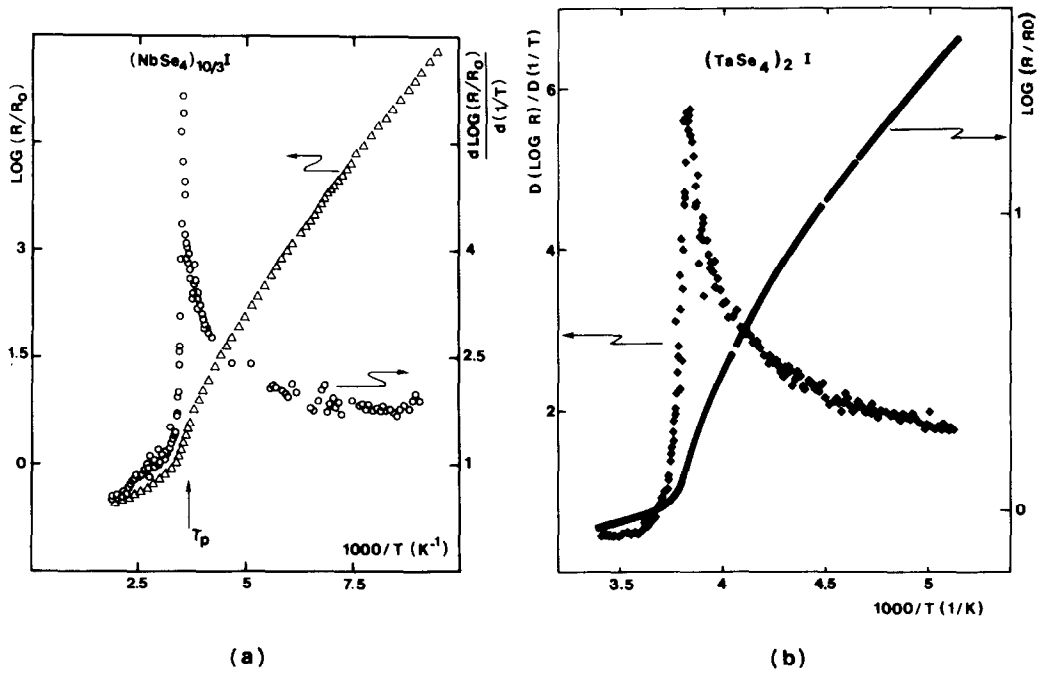

FIG. 6. CDW transition in (a) $(NbSe_4)_{10/3}I$ and (b) $(TaSe_4)_2I$.

tained. In the nonlinear regime the current is the sum of an ohmic contribution and a contribution due to the moving of the CDW with velocity v:

$$J = J_{ohm} + nev,$$

where ne is the electronic concentration in the bands affected by the CDW gap. The velocity v can be written as $v = \lambda\nu$ with $\lambda = 2\pi/q$ that we have already measured. ν is manifested under the form of a periodic noise that can be decomposed in a fundamental and its harmonic. ν is displaced toward higher values when the field increases. By measuring J_{CDW} it is possible to check (Fig. 7a) the linear relationship between J_{CDW} and ν:

$$J_{CDW} = (ne\lambda)\nu$$

$(NbSe_4)_{10/3}I$ shows similar effects below 285 K. But, in addition an hysteresis phenomenon (Fig. 7b) takes place in the 285–220 K temperature range (*18*). This type of memory effect, also observed in orthorhombic TaS_3 (*19*) and in the blue bronze $K_{0.30}MoO_3$ (*20*) depends on the electrical history of the sample. It implies that probably closely related metastable states of comparable energy are involved in pinning effects. We have one threshold field when the field is increased and a different one when it is decreased.

All these striking physical effects are an important justification of the work done to imagine and prepare these compounds. But charge density waves may also be expressed with classical chemical concepts. When the electronic density increases between ions we have a true picture of a chemical bond. On the opposite the diminution of electronic density, related to a lengthening of the ion–ion distance, can go as far as an absence of direct interaction. This chemical approach has lead to an illus-

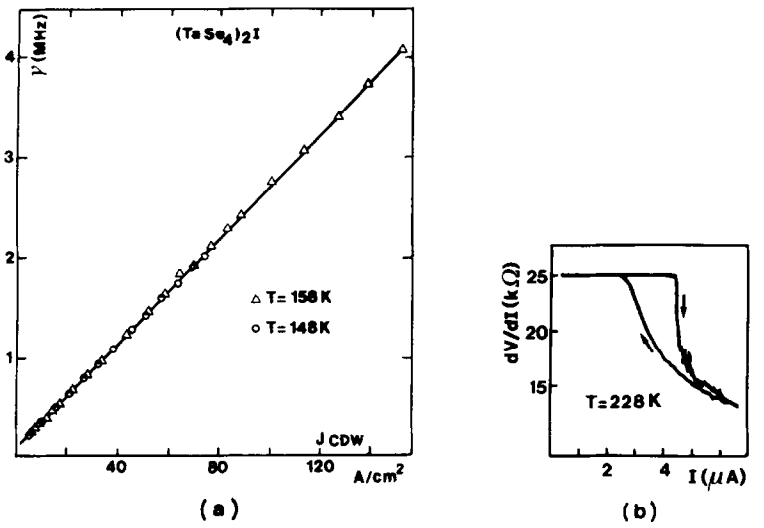

FIG. 7. (a) Linear relationship between J_{CDW} and ν in $(TaSe_4)_2I$, (b) memory effect in the nonohmic behavior of $(NbSe_4)_{10/3}I$.

tration of the phenomena through an image of waves of bonds distribution. The $(MSe_4)_n$-halogen phases represent a nice illustration of this concept.

Like transition metal trichalcogenides, the $(MX_4)_nY$ phases are obtained in sealed tubes, i.e., under thermodynamic conditions that are not well defined. A small range of temperature is associated with particular starting conditions (quantities of elements, volume of the tube) in order to get a given compound. In addition the structural similarity of all the compounds with only slight changes in the iodine repartition and in the metallic sequence along the chains makes it possible to observe intergrowth phenomena. This is probably the case for some crystals of $(NbSe_4)_3I$ presenting at low temperature an electrical behavior which would be expected if $(NbSe_4)_{3.33}I$ microdomains are present along the chains. Without any modification of the structural framework this would essentially result in different local arrangements of the iodine ions. It sheds also some light on the real nature of defects pinning charge density waves. As well as in trichalcogenides there is a high probability that such defects are not represented by chemical impurities but also by chemical defects such as local variations of the Se—Se bond lengths or structural defects due to intergrowth mechanisms.

IV. New Developments

The $(MX_4)_n$-halogen phases have been essentially limited to those containing iodine. A few compounds with bromine were characterized. There was however a double interest to go up the halogens group to obtain derivatives with bromine and chlorine.

First, it can be forecast that if the structural type is maintained, it will be less stable, and it is in fact the reason why these phases are not easily formed. In effect, the chains would then have a higher overall charge, the halogen being itself more electronegative. In addition, the smaller size of the halogen would not minimize the repulsions by sufficiently separating the chains.

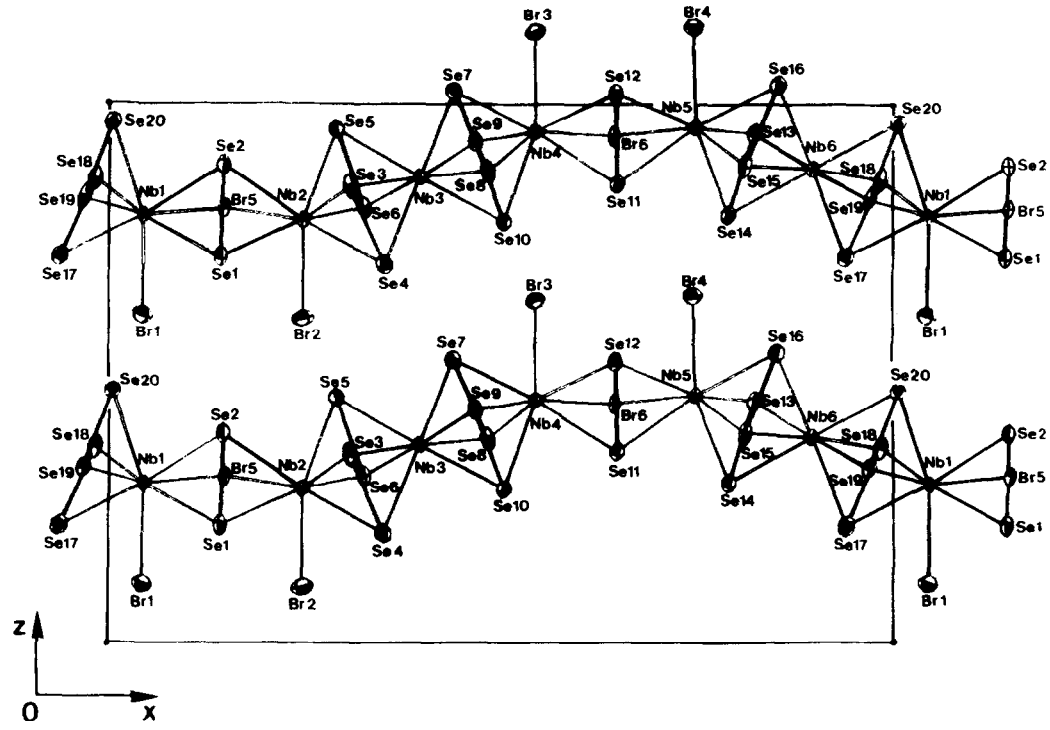

FIG. 8. Structural type of $Nb_6Se_{20}Br_6$.

It would probably be possible to solubilize the $(NbX_4)_\infty$ chains in appropriate solvents, following the work performed by Tarascon and di Salvo (*21*) on the $M_2Mo_6Se_6$ (M = Li, Na, K) phases.

The second direction of possible development results from the fact that as the halogen becomes more electronegative, it will tend to become closer to niobium by pushing apart the selenium framework. This has been realized in various new compounds such as, for example, $Nb_6Se_{20}Br_6$ which is a good illustration of this idea (*22*). This material has a one-dimensional structure rather exceptional with sinusoidally modulated chains (Fig. 8). Within one wavelength there are six niobium-niobium distances with the following sequence of two groups of two short and one long Nb—Nb distances:

$$Nb_1 \overset{3.91}{—} Nb_2 \overset{3.09}{—} Nb_3 \overset{3.09}{—} Nb_4 \overset{3.94}{—} Nb_5 \overset{3.07}{—} Nb_6 \overset{3.10}{—} Nb_1$$

Bromine atoms are coordinated to Nb_1 and Nb_2, then Nb_4 and Nb_5. Rectangular planes of two $(Se_2)^{2-}$ groups are perpendicular to the Nb_2—Nb_3 and Nb_3—Nb_4 axis (portion of three aligned Nb). The same feature is observed for the Nb_5—Nb_6—Nb_1 alignment. This provides a rectangular antiprismatic arrangement of Se atoms around Nb_3 and Nb_6. The bromine atoms are also responsible of a linking between adjacent chains through short Br—Se bondings (Br_3—Se_{10} = 3.629 Å, for example).

Structural analogies appear clearly with other 1D compounds of niobium and tantalum. They are based on the presence of similar building groups of the chains and the regular change of their gathering from one compound to another. $Nb_6Se_{20}Br_6$ is to

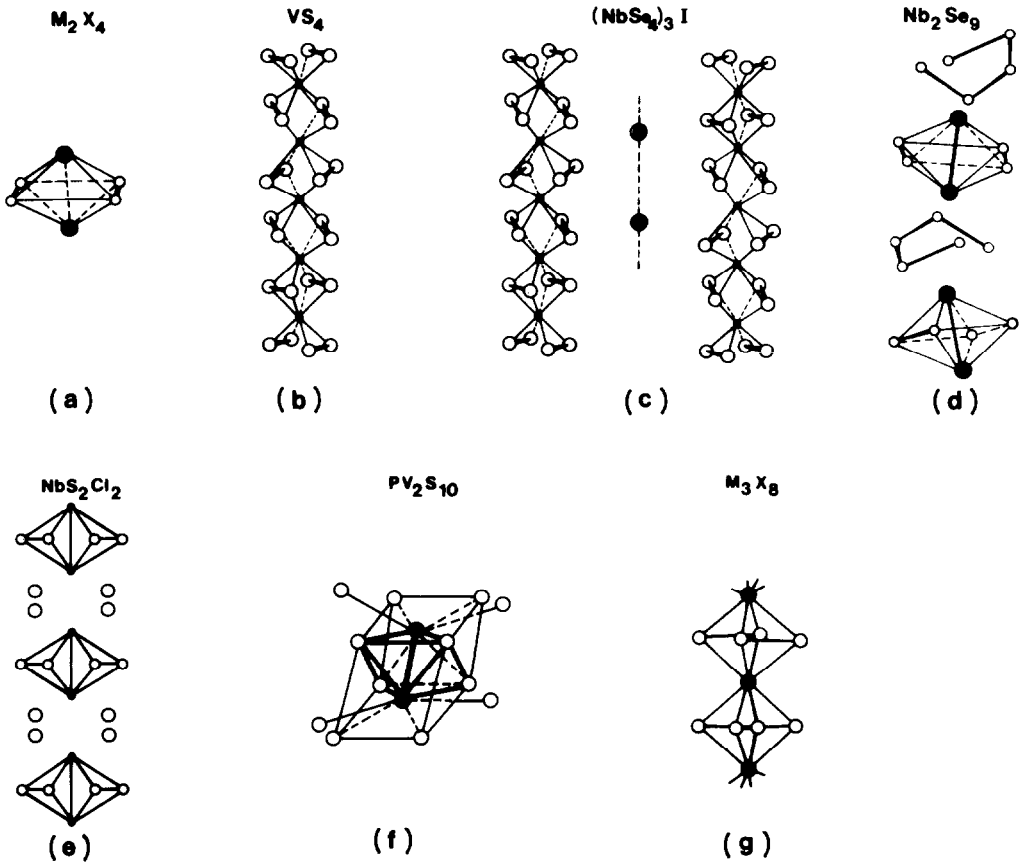

FIG. 9. Nb_2X_4 groups (a), as building units in VS_4 (b), $(NbSe_4)_3I$ (c), Nb_2Se_9 (d), NbS_2Cl_2 (e), M_2S_{12} entities in PM_2S_{10} structures (f), Nb_3Se_8 entities in $Nb_6Se_{20}Br_6$ (g).

be compared to niobiuim phases with a rectangular antiprismatic coordination. The basic arrangement in these networks is the double pyramid Nb_2Se_4 or Nb_2S_4 (Fig. 9). This arrangement exists as isolated groups in NbS_2Cl_2 (*23*) in which the Nb_2S_4 bipyramids are separated by chlorines. It is found again in Nb_2Se_9 (*24*) in which this time Se_5 polyanions are found between the Nb_2Se_4 groups and in such phases as PV_2S_{10}, PNb_2S_{10}, and P_2NbS_8 compounds reported by Brec *et al.* (*25, 26*). Infinite condensation of M_2X_4 bipyramids lead to MX_4 chains that are found alone in VS_4 or separated by halogens columns in the $(NbSe_4)_nI$ series.

Nb_2Se_4 groups are associated to form Nb_3Se_8 units in $Nb_6Se_{20}Br_6$. In these units terminal niobium atoms are bonded to bromine atoms. We find then here an intermediary situation between the case of isolated bipyramids and that of infinite condensation which are the only situations known previously. A new compound studied presently in our group seems to correspond to the next step of condensation with four metal atoms associated in a Ta_4Se_{12} group. Many new compounds can be predicted in such a situation. It is clear also that pressure effect should induce phase transitions related to new sequences of distances inside the chains and a possible nonmetal-to-metal transition.

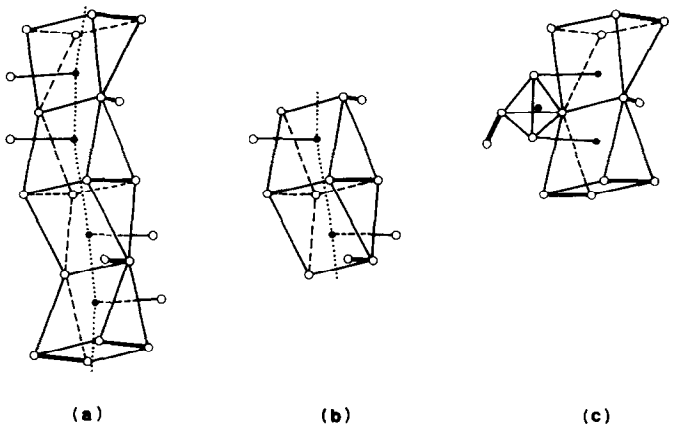

FIG. 10. (a) Infinite M_2S_9 chains from bicapped M_2S_{12} biprisms (b). Position of the PS_4 tetrahedra connecting chains (c).

V. 1D Conductors as Host Structures in Intercalation Chemistry

The driving force for intercalation chemistry is to be found in a favorable competition between the two main energy terms which are the cost in elastic energy associated with the host distortion when intercalation takes place and the gain in electronic energy due to the difference between the initial and final energy levels of the transferred electrons. Of course other terms, and particularly configurational entropy, ion–electron interactions, are to be considered. But they are quite corrective terms as compared to the two others. The accepting level in the host structure can be a discrete atomic level, such as Fe^{3+} reduced to Fe^{2+} in FeOCl (which does not exclude some hopping mechanism according to temperature). It can be represented by molecular levels of a polyatomic entity existing in the structure such as in the Mo_6 clusters of Chevrel phases (which fix the number of electrons to be accepted, i.e., the number of associated ions: 4Li, 2Zn . . .). Finally the electron can be delocalized in the conduction band of the host: in that case things may be very different depending on the width or population of the band.

Another situation is represented by the case in which the transferred electron would be accepted by a polyanionic species, the $(Se_2)^{2-}$ group, for example.

A reversible mechanism would be associated with an elastic variation of the S—S length in the redox process

$$(S_2)^{2-} + 2e^- \rightleftharpoons 2S^{2-}$$

The reversible increase and decrease in S—S distance will operate in the case of S_2^{2-} pairs situated at the edges of 1D skeletons.

In niobium and tantalum chemistry as we have seen S_2^{2-} or Se_2^{2-} pairs begin to appear in the MX_n formula when n becomes larger than 2. One leaves the layered models MS_2 or MSe_2 to obtain for example $NbSe_3$ with one $(Se_2)^{2-}$ pair, $NbSe_4$ with two pairs, Nb_2Se_9 with a complex (Se_5) group. Considering sulfur–phosphorus and transition metal systems, we found that one leaves also the layered MPS_3 phases to get new low-dimensional, and, in particular, 1D compounds presenting $(S_2)^{2-}$ pairs. These latter phases are noteworthy new systems for intercalation. The numerous S—S pairs constitute as many redox centers located at the chain edges, and because of an ex-

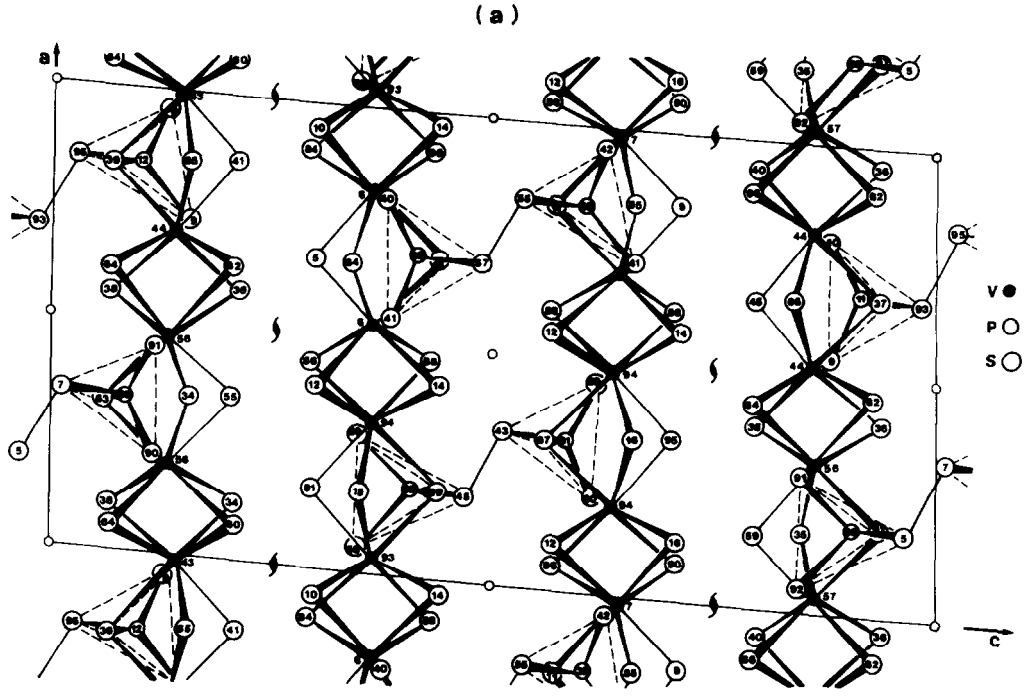

FIG. 11. PV_2S_{10} (a), PNb_2S_{10} (b), $PNb_2S_{10.5}$ (c) structures with one-dimensional and two-dimensional arrangements of (M_2S_9) chains linked by PS_4 tetrahedra (a, b) or by a P_2S_9 group (c).

pected good elasticity, should lead to fair reversibility.

PV_2S_{10}, PNb_2S_{10}, $PNb_2S_{10.5}$ ($P_2Nb_4S_{21}$) are some typical members of that series of derivatives (*25, 26*). They all utilize as building units bicapped M_2S_{12} biprisms with a metal–metal bond inside. All the biprisms are bonded together to form infinite M_2S_9 chains (Fig. 10). Then the bonding between these chains takes place through [PS_4] units. The way such bondings are made determine the dimensionality of the phases which is

- 1D (PV_2S_{10}) when the [M_2S_9] lines are linked two by two (Fig. 11a).
- 2D (PNb_2S_{10}) when the [PS_4] groups link the chains on both their sides (Fig. 11b).
- 2D ($PNb_2S_{10.5}$) when the phosphorus sulfide groups link the chains above and sideway to each other in a type of step-linking (Fig. 11c).

The occurrence of the last structural type is made possible by the extra half-sulfur atom which constitutes longer P_2S_9 ($S_3P(S—S—S)PS_3$) linking groups, whereas only P_2S_8 ($S_3P(S—S)PS_3$) linking units are found in PV_2S_{10} and PNb_2S_{10}.

With respect to such structural arrangement higher sulfur content results in anionic catenation with the occurrence of $(S_3)^{2-}$ anions in addition to the S_2^{2-} and S^{2-} species already present in the structures. This aspect constitutes a first approach toward the separation of functions, toward composite structures with some elements determining the frame in which intercalation takes place whereas some others constitute redox centers.

$P_4Ta_4S_{29}$, recently characterized (*27*), may represent an illustration of that idea. The structure is built from the same M_2S_{12} biprisms and PS_4 tetrahedra which enclose

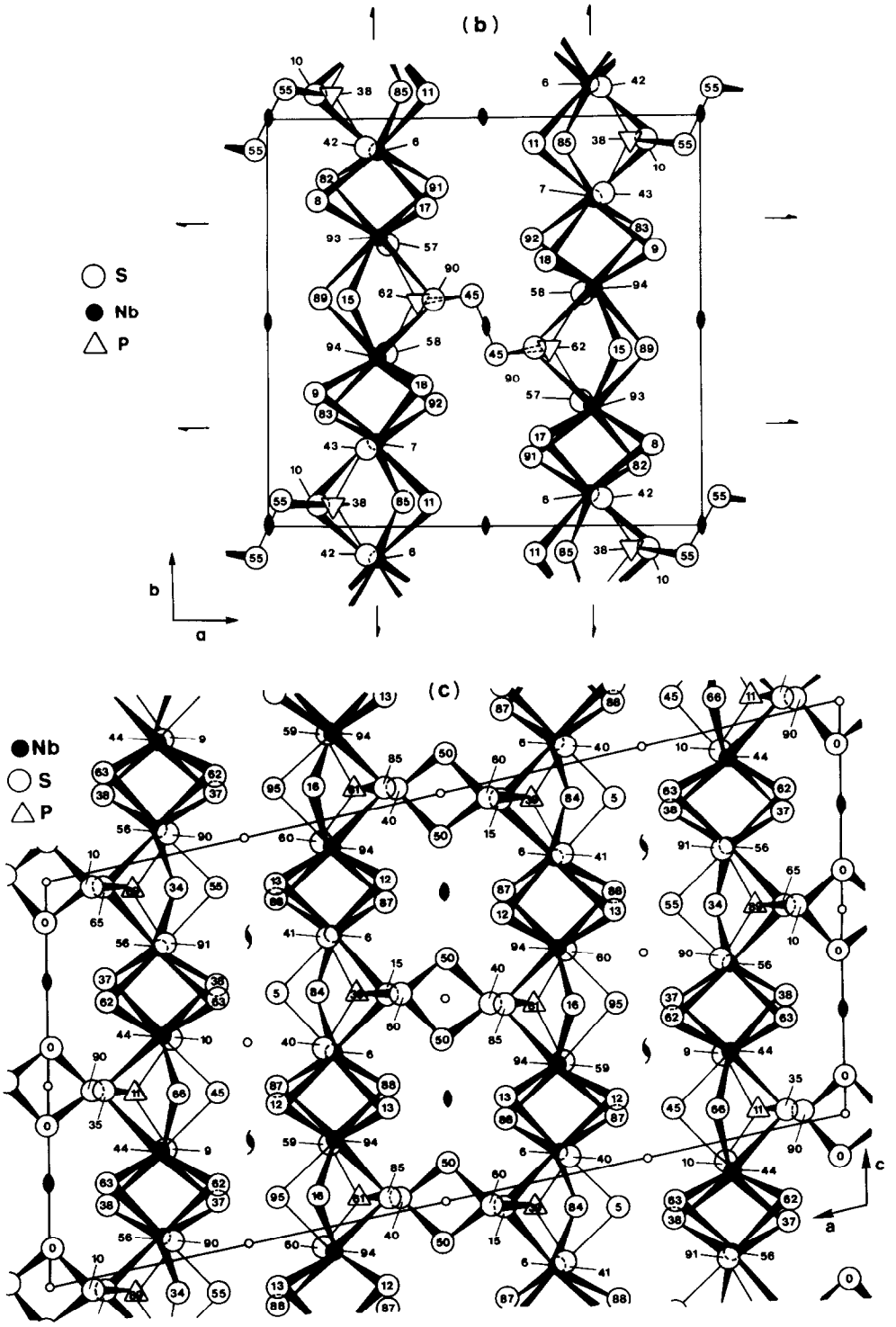

FIG. 11—*Continued.*

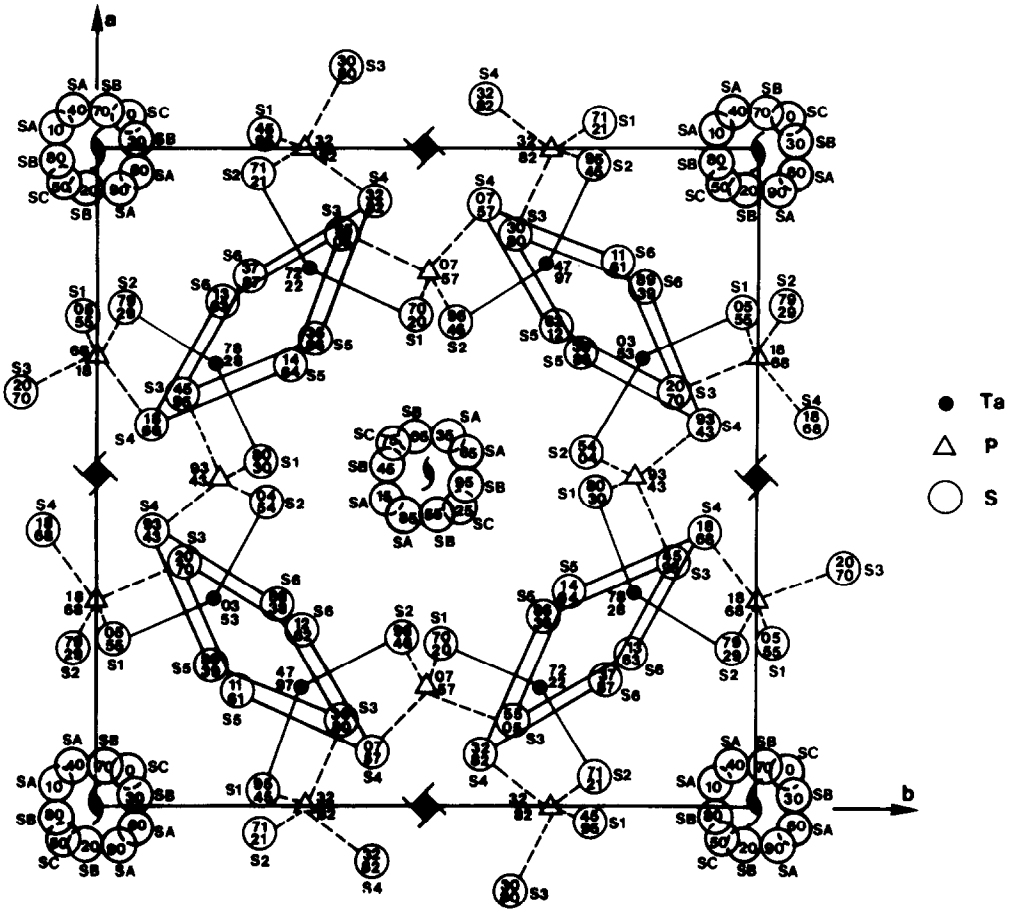

FIG. 12. $P_4Ta_4S_{29}$ structural type.

large tunnels containing long chains of polymeric sulfur (Fig. 12).

References

1. F. JELLINEK *in* "Inorganic Sulfur Chemistry" (G. Nickless, Ed.), Elsevier, Amsterdam (1968).
2. A. MEERSCHAUT AND J. ROUXEL, *J. Less-Common Met.* **39,** 498 (1975).
3. F. DI SALVO, *Adv. Phys.* **24-2,** 117 (1975).
4. P. MONCEAU, N. P. ONG, A. M. PORTIS, A. MEERSCHAUT, AND J. ROUXEL, *Phys. Rev. Lett.* **10,** 602 (1976).
5. T. J. WIETING, A. GRISEL, AND F. LEVY, *Mol. Cryst. Liq. Cryst.* **81,** 117 (1982).
6. E. BJERKELUND AND A. KJEKSHUS, *Z. Anorg. Allg. Chem. B* **328,** 235 (1964).
7. T. SAMBONGI, K. TSUTSUMI, Y. SHIOZAKI, M. YANAMOTO, K. YAMAYA, AND Y. ABE, *Solid State Commun.* **22,** 729 (1977).
8. C. ROUCAU, R. AYROLES, P. MONCEAU, L. GUEMAS, A. MEERSCHAUT, AND J. ROUXEL, *Phys. Status Solidi* **62,** 483 (1980).
9. A. MEERSCHAUT, P. GRESSIER, L. GUEMAS, AND J. ROUXEL, *Mater. Res. Bull.* **16,** 1035 (1981); R. J. CAVA, V. L. HINES, A. D. MIGHELL, AND R. S. ROTH, *Phys. Rev. B* **24-6,** 3634 (1981).
10. D. A. KESZLER AND J. A. IBERS, *J. Solid State Chem.* **52,** 73 (1984).
11. R. CLEMENT, *J. Chem. Soc. Chem. Commun.*, 647 (1980).
12. P. GRESSIER, A. MEERSCHAUT, L. GUEMAS, J.

ROUXEL, AND P. MONCEAU, *J. Solid State Chem.* **51,** 141 (1984).
13. P. GRESSIER, M.-H. WHANGBO, A. MEERSCHAUT, AND J. ROUXEL, *Inorg. Chem.* **23,** 1221 (1984).
14. C. ROUCAU, R. AYROLES, P. GRESSIER, AND A. MEERSCHAUT, *J. Phys. C, Solid State Phys.* **17,** 2993 (1984).
15. H. FUJISHITA, M. SATO, AND S. HOSHINO, *Solid State Commun.* **49-4,** 313 (1984).
16. Z. Z. WANG, M. C. SAINT LAGER, P. MONCEAU, M. RENARD, P. GRESSIER, A. MEERSCHAUT, AND J. ROUXEL, *Solid State Commun.* **46-4,** 325 (1983).
17. M. MAKI, M. KAISER, A. ZETTL, AND G. GRÜNER, *Solid State Commun.* **46,** 497 (1983).
18. Z. Z. WANG, P. MONCEAU, M. RENARD, P. GRESSIER, L. GUEMAS, AND A. MEERSCHAUT, *Solid State Commun.* **47-6,** 439 (1983).
19. G. MIHALY AND L. MIHALY, *Solid State Commun.* **48,** 449 (1983).
20. J. DUMAS, C. ESCRIBE-FILIPPINI, J. MARCUS, AND C. SCHLENKER, "Nato-Davy Advanced Institute: Electrons and Ions in Condensed Matter," Cambridge Univ. Press, London/New York (1983); R. M. FLEMING AND L. F. SCHNEEMEYER, *Phys. Rev. B* **28-12,** 6996 (1983).
21. J. M. TARASCON AND F. J. DI SALVO, *J. Solid State Chem.* in press.
22. P. GRENOUILLEAU, A. MEERSCHAUT, AND J. ROUXEL, *J. Solid State Chem.* in press.
23. J. RIJNSDORP, G. J. DELANGE, AND G. A. WIEGERS, *J. Solid State Chem.* **30,** 365 (1979).
24. A. MEERSCHAUT, L. GUEMAS, R. BERGER, AND J. ROUXEL, *Acta Crystallogr. Sect. B* **35,** 1747 (1979).
25. R. BREC, G. OUVRARD, M. EVAIN, AND J. ROUXEL, *J. Solid State Chem.* **47,** 174 (1983).
26. P. GRENOUILLEAU, R. BREC, M. EVAIN, AND J. ROUXEL, *Rev. Chim. Min.* **20,** 628 (1983).
27. M. EVAIN, M. QUEIGNEC, R. BREC, AND J. ROUXEL, *J. Solid State Chem.* **56-2,** 148 (1985).